

Article

Multidisciplinary Study of the Rybachya Core in the North Caspian Sea during the Holocene

Alina Berdnikova ^{1,2,*} , Elena Lysenko ¹, Radik Makshaev ^{1,2}, Maria Zenina ³ and Tamara Yanina ^{1,2}

¹ Paleogeography Laboratory of Recent and Pleistocene Sediments, Faculty of Geography, Lomonosov Moscow State University, 119991 Moscow, Russia

² Laboratory of Macroecology and Biogeography of Invertebrates, Saint Petersburg State University, 199034 Saint Petersburg, Russia

³ P.P. Shirshov Institute of Oceanology, Russian Academy of Science, 117997 Moscow, Russia

* Correspondence: alinaberdnikowa@yandex.ru

Abstract: Mollusk fauna is an important component of the Caspian Sea ecosystem alongside ostracods and diatoms. These faunal proxies are essential indicators of hydrological shifts reflecting global and regional climate changes. Adding lithological, geochemical, and geochronological (radiocarbon) data, we revealed paleogeographic events of different scales recorded in the sequence of the Rybachya core from the North Caspian Sea. Here, we present the reconstruction of Mangyshlak paleovalley sediments during the Holocene multi-stage Neocaspian transgression, reflecting global and regional climate changes varying in scale and direction. The determined age of paleovalley-fill sediments, 8070 ± 110 cal yr BP and 7020 ± 140 cal yr BP, suggests that sedimentation processes with extended warming and humidification started later and lasted longer than was assumed earlier. Biological proxies indicate quasi-cyclic variability and shifts from brackish to freshwater conditions throughout the studied interval. Rybachya core was obtained from the early Khvalynian deposits. The Mangyshlak flow formed the depression and eroded the late Khvalynian deposits, which we did not observe in the core structure. It possibly collapsed into paleodepression and acted as a host material for the freshwater lentic faunal association. During the Holocene, we detected a transition from a tranquil water regime to a more dynamic one during the paleovalley gradual filling, followed by marine conditions typical for the modern Caspian Sea.

Keywords: paleovalley; Caspian Sea; Holocene; Neocaspian; Mangyshlak; mollusk fauna; diatoms; ostracoda; biostratigraphy; climate changes



Citation: Berdnikova, A.; Lysenko, E.; Makshaev, R.; Zenina, M.; Yanina, T. Multidisciplinary Study of the Rybachya Core in the North Caspian Sea during the Holocene. *Diversity* **2023**, *15*, 150. <https://doi.org/10.3390/d15020150>

Academic Editors: Maxim V. Vinarski and Rodrigo Salvador

Received: 26 October 2022

Revised: 13 January 2023

Accepted: 17 January 2023

Published: 21 January 2023



Copyright: © 2023 by the authors. Licensee MDPI, Basel, Switzerland. This article is an open access article distributed under the terms and conditions of the Creative Commons Attribution (CC BY) license (<https://creativecommons.org/licenses/by/4.0/>).

1. Introduction

The Caspian Sea is the world's largest endorheic inland basin in terms of area and volume. It consists of three basins, deepening southwards. We focused our research on the northern, smallest (about 90,000 km²) basin of the sea, with an average depth of 5–6 m and a maximum of 15–20 m [1]. A shallow extension of the central basin, its boundary runs along the Mangyshlak threshold from the Tyub-Karagan Peninsula to the Kulalinskaya Bank and further west to the Chechen Island (Figure 1). The modern North Caspian has a temperate continental climate. The maximum annual temperature range in August is 25–26 °C, while the lowest February temperatures go down to 0–0.5 °C [2]. The salinity of the North Caspian Sea ranges from 1 to 3‰ near the delta of the Volga River to 11‰ (the average of the rest of the northern basin). In winter, the salinity is higher (~13‰) because of ice formation. Most water (~80%) and terrigenous material derive in the North Caspian from the Volga River [3–5]. Its avandelta is an important element of the bottom topography, typically flat and shallow with a system of channels and mouth bars. After more than a century of Caspian Sea research, there is not yet a full understanding of the causes of the water level fluctuations and the dynamics of the water circulation in the Caspian Sea in the past [6–12]. Its level has changed significantly over various timescales, leading to

rapid variations in the volume and area of the water body, which is especially important in the shallow northern part. Since the shelf area was exposed during a regressive stage or low-standing periods, land and freshwater mollusk communities and other organisms settled in this area, indicating climate change both in the Caspian Sea region and the East European Plain [13]. Proxies such as mollusk fauna, ostracods and diatoms are an important component of the Caspian ecosystem and are essential indicators of hydrological shifts reflecting global and regional climate changes traced step-by-step in this work [13–17].

The main reason for the Caspian Sea-level changes during the Holocene is believed to be climate-induced fluctuations; however, the data on the extent of these changes is controversial so far. Several published works [7,11,18,19] provide sea-level curves that do not agree with each other and have a considerable range of differences. During the last century, analyses of the available data on the discharge to the sea and the observed sea-level fluctuations suggest that climatically driven changes of the river inflow are the major causes for sea level fluctuations, although plenty of issues remain debatable [4–10,12,14].

The Late Pleistocene and Holocene in the Caspian Sea region are represented by Khvalynian and Neocaspian (also known as Novocaspian or Newcaspien) stages, respectively [20–22]. Long-established Caspian paleogeographic events during the Holocene include the Mangyshlak regressive and Neocaspian transgressive epochs [7,18,19,23,24]. The Neocaspian stage was preceded by the Khvalynian stage, which comprises Lower and Upper Khvalynian horizons [25].

Andrusov N.I. [26] defined the Khvalynian horizon after discovering the endemic bivalve mollusk species *Didacna* Eichw. [27]. In the 1950s–1960s, after geomorphological and sedimentological studies of several key sections, the Khvalynian stage was divided into the lower Khvalynian and upper Khvalynian subhorizons that correspond to transgressive events with different sediment composition and mollusk assemblages, such as *Didacna protracta* (Eichwald, 1841), *D. parallela* (Bogachev, 1932), *D. praetrigonoides* (Nalivkin and Anisimov, 1914), *D. ebersini* (Fedorov, 1953), *D. cristata* (Bogachev, 1932), *Monodacna caspia* (Eichwald, 1829), *Dreissena rostriformis distincta* (Andrusov, 1897), and *Hypanis plicata* (Eichwald, 1829) [14,28].

Bogachev V.V. [29] defined the Neocaspian stage. Neocaspian deposits overlay Khvalynian sediments and correspond to transgressive series that reached –20 m asl (above sea level). The Neocaspian mollusk assemblages contained *Didacna crassa* (Eichwald, 1829), *D. baeri* (Grimm, 1877), *D. pyramidata* (Grimm, 1877), *D. longipes* (Grimm, 1877), *D. trigonoides* (Pallas, 1771), *D. barbotdemarnii* (Grimm, 1877), *Monodacna caspia*, *Adacna vitrea* (Eichwald, 1829), and an invasive species of *Cerastoderma glaucum* (Bruguère, 1789) [14,28].

The age of the Neocaspian transgression and its stages have been a subject of comprehensive discussion based on radiocarbon age data and historical materials [6,30–32]. Most researchers agree on an age of 8 kyr BP and younger [6,7,32,33]. Krijgsman W. et al. [22] summarized data on the Holocene Caspian Sea regional stages and global chronostratigraphic units for the Pontocaspian region.

The Neocaspian and Late Khvalynian transgressive stages are separated by the Mangyshlak regressive event, when sea-level dropped to –80 m asl [6]. Seismic data show that the Mangyshlak deposits fill paleovalleys in the strata of the Khvalynian deposits and occur only within the limits of the existing sea area [19,32]. Bezrodnikh Y.P. and Sorokin V.M. [19] describe paleovalleys as “elongated, stretching in the east-west direction for a few kilometers almost parallel to each other, typically 300–500 m wide and 6–8 m deep, locally attaining 12–13 m deep depressions”. Such paleovalleys are detected on seismic profiles but are not reflected in the seabed relief over a large distance. In the North Caspian Sea, the largest area of deposition during the Mangyshlak regression was the Volga paleovalley (Figure 1), stretching southeast to the large alluvial fan flanking the Middle Caspian depression. For smaller scale paleovalleys, the following characteristics are given [19]: widespread to the west and to the east from the Volga paleovalley (Figure 1) at water depths up to 20 m below present Caspian Sea level; the features of a paleovalley appear as a gently sloping hollow to the south; heterogenous structure to the succession of sediments that

completely fill the paleovalley; dynamic sedimentary environments and facies changes during paleovalley aggradation. The incised paleovalleys are evident in seven seismic profiles crossing Volga paleovalley over a longitudinal distance of ~90 km [19].

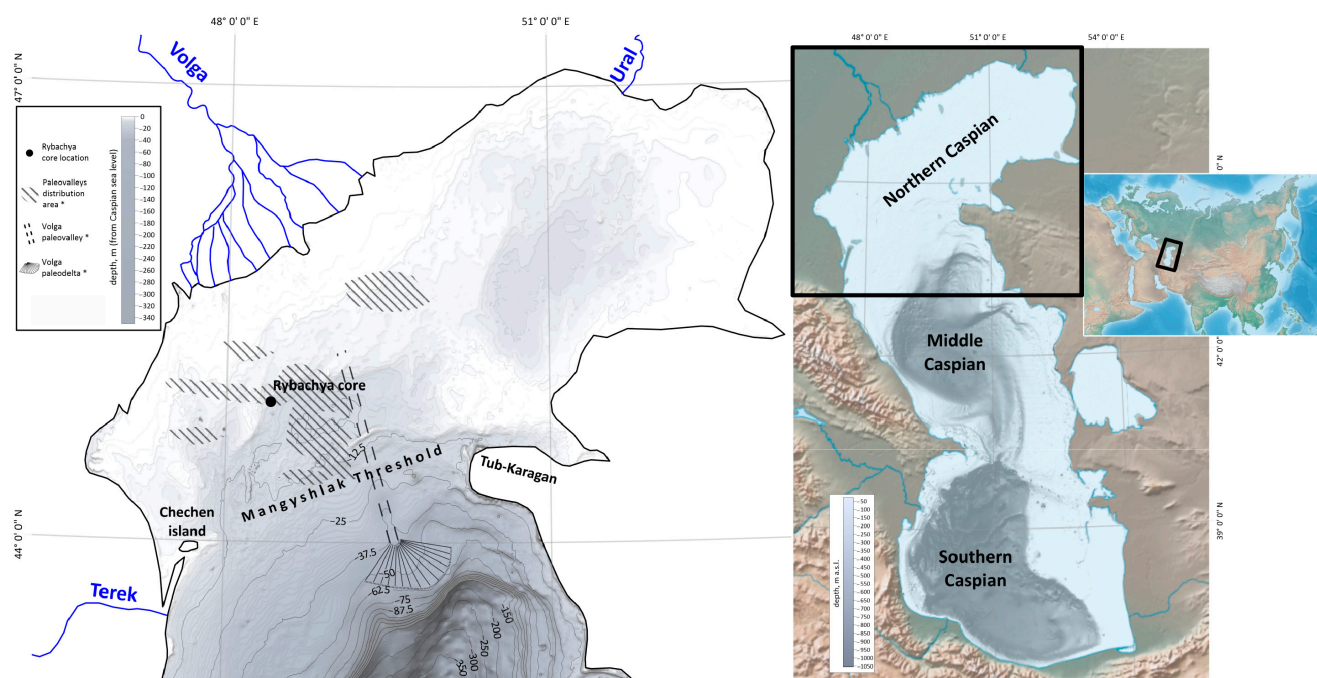


Figure 1. Geographic location of the studied Rybachya core (the bottom surface is hill-shaded). * According to Bezrodnikh and Sorokin, 2016 [19].

In this study, we used drilling material from the northern region to study freshwater and brackish water faunal associations to reconstruct and characterize the development in this part of the basin during the Holocene. Our results have led to the assumption that the Rybachya core was located within a paleovalley widespread in the North Caspian.

2. Materials and Methods

The Rybachya core was recovered during the prospecting survey in 2014 in the Rybachya region of the North Caspian area at a water depth of 8 m. Since the prospecting survey targeted oil-gas exploration, we cannot reveal the core coordinates, but the location is shown in Figure 1.

The core was stored intact and covered in paraffin in the Paleogeography Laboratory of Recent and Pleistocene Sediments (Lomonosov Moscow State University). Reported analyses were carried out during 2020–2021.

The total length of the retrieved core is 9.5 m. We have very few samples from the 6.4–9.5 m interval, but grain size and geochemical data from this interval are very helpful for our understanding of the paleogeography and sedimentation history of the Rybachya core. There were no faunal nor floral remains below 6.4 m; thus, our study focused on the upper 6.4 m of the core. Biostratigraphic zones or assemblages were established on the basis of qualitative and quantitative changes observed in the core using the data on taxonomic diversity, dominant species, concentration of valves (available only for diatoms, mln valves/g of air-dried sediment), and ecological characteristics of the species [13,14]. These assemblages represent lifetime ecological communities. Therefore, the biostratigraphic zones we established here are ecological zones or ecozones [25]. Here, we report the results of the multi-proxy analysis of the core samples from this site.

2.1. Grain Size Analysis

We analyzed nine samples from the Rybachaya core from the <1 mm size fraction using the “Fritsch Analysette 22” laser diffraction grain size analyzer. All samples were dried at 50 °C for 3 h and then pretreated with 10% hydrochloric acid (HCl) and hydrogen peroxide (H₂O₂) to remove carbonates and organic particles. To avoid coagulation, sodium pyrophosphate 5% (Na₄O₇P₂) was added to the samples as a dispersion agent. The measurements were carried out with two lasers from 0.8 to 2000 μm three times for 4 min each. Grain size classes were identified according to the Kachinskiy classification [34], defined as: <1 μm (clay); 1–5 μm (fine silt); 5–10 μm (medium silt); 10–50 μm (coarse silt); 50–250 μm (fine sand); and 250–1000 μm (medium and coarse sand) [34–36]. There were no coarser fractions found at this site. Grain size and geochemical results are shown in Figure 2.

2.2. Geochemical Analyses

We used the Olympus Delta Professional analyzer to perform Energy Dispersive X-ray Fluorescence (EDXRF) geochemical analyses on nine bulk samples. Results for Si, Ca, Sr, Fe, and Ti are presented in Table 1 and Figure 2.

2.3. Mollusk Fauna Analysis

We analyzed thirteen samples (Figure 4) containing 960 mollusk remains. The analysis included mollusks’ taxonomic identification and preservation. We studied mollusk fossils for signs of dissolution, abrasion, color preservation, and fragmentation. The findings of articulated bivalves pointed to in situ samples. The data provided the basis for the biostratigraphic subdivision of the sedimentary series and paleobasin reconstruction. Paleoreconstruction is based on the interpretation of the alternating marine, brackish water, slightly brackish water, freshwater, and terrestrial assemblages of mollusks. We focused on the bivalve genus *Didacna* Eichwald [27], an index fossil for the Caspian Sea [13,25,37]. We used the available ecological data (salinity, depth range, and habitat) to reconstruct the Holocene environment of the Northern Caspian [13].

2.4. Diatom Analysis

The samples for diatom analysis came from all lithological units, with a total of nine samples analyzed (Figures 5 and 6). All the samples were air-dried before preparation and then treated using standard methods [38]. Approximately 5 g of dry material was taken from silty units and 20 g from sandy layers. To remove organic matter and carbonates, each sample was put into a heat-resistant glass and boiled in 400 mL of 10% H₂O₂ for 1.5 h. Next, all the coarse and silty matter was gradually removed by elutriation. We used a 1 mL pipette to place the suspension containing diatoms on a clean, dry coverslip to dry at room temperature. Coverslips were mounted in Naphrax, put on the slides, and studied at 1000× under a Carl Zeiss Jena JENAVAL light microscope with an oil immersion objective. Diatom taxonomic species-level identification was based on Krammer and Lange-Bertalot [39–42] and Zabelina et al. [43].

2.5. Ostracod Analysis

We analyzed twelve samples of ostracods (Figures 7–9) using standard methods [44–46]. Samples were soaked for one hour to disaggregate the sediment and then washed through a 63 μm sieve, and the remaining fraction was air-dried. The 0.1–2 mm and 0.063–0.1 mm dry fractions were analyzed using a binocular microscope. Ostracod valves were identified to species level when possible [16,47–49]. Picked specimens were placed and stored in plastic single-cell slides.

2.6. Radiocarbon Dating

Radiocarbon dates on mollusk shells (*Monodacna caspia* and *Dreissena polymorpha* (Pallas, 1771)) were obtained from two intervals (1.73–1.96 m and 2.07–2.11 m). The samples were processed at the Radiocarbon Laboratory of St. Petersburg State University (index LU),

and the liquid scintillation technique [50] was used. The radiocarbon age was calibrated using OxCal 4.4.4 software [51] and the IntCal20 calibration curve [52].

Data obtained by the scintillation method did not include a correction for isotope fractionation. Therefore, we relied on the concept proposed by Karpychev Yu.A. [53] that the reservoir effect for the Caspian Sea estimated from mollusk shells and seal bones is 380–440 years [54]. The value of $\delta^{13}\text{C}$ required for corrections for Caspian mollusk shells isotope fractionation varies from -2.5 to 0‰ . The correction for isotope fractionation is needed if it differs from the VPDB (Vienna Pee Dee Belemnite) standard (-25‰). A value of 1‰ corresponds to 16 radiocarbon years. Adding to the obtained radiocarbon age the value of the correction for isotope fractionation (about 360–410 years for Caspian shells), it is also necessary to subtract the value of the reservoir effect (about 380–440 years). It allows us to not apply a correction for the reservoir effect and use the IntCal20 calibration curve. The calibrated ages are presented with a 2σ deviation.

3. Results

3.1. Grain Size Analysis

Five groups of samples were distinguished (Figure 2).

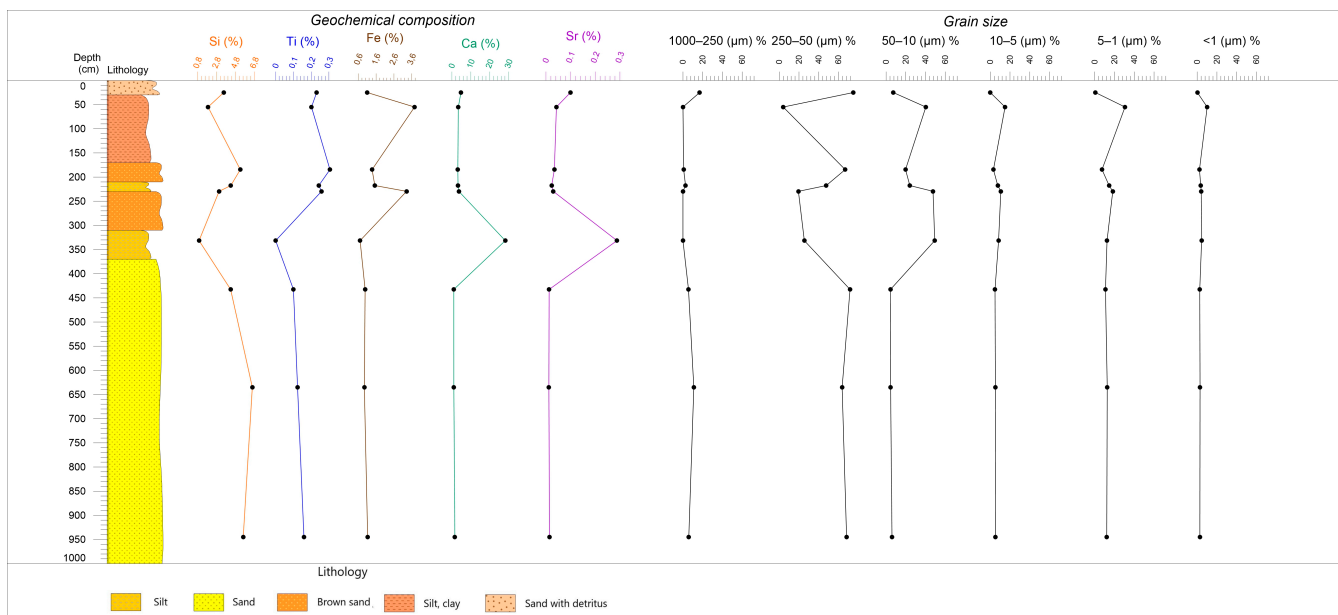


Figure 2. Grain size and geochemical analysis results of the studied Rybachya core.

The first group includes samples of the basal lithological unit collected at depths of 9.4–9.5 m, 6.3–6.4 m, and 4.2–4.4 m (Figure 2). We observed a bimodal distribution of particle size in this unit. Fine sand represents the majority (about 60–70%) of the sediment content, while fine silt takes up about 11–13%.

The samples from intervals of 3.0–3.5 m and 2.2–2.3 m represent the second group. It shows a bimodal particle size distribution with more fine sediment content: coarse silt averages 48%, while fine silt makes up 15%. Medium silt averages 10% of the sediment content as well.

The third group includes the samples from intervals of 2.1–2.2 m and 1.7–2.0 m. The basal layer contains a significant amount of fine sand whose percentage rises upwards from 48% to 67%. The peak of fine sand is less symmetric due to the admixture of coarse silt (up to 24%).

The sample at a depth of 0.3–0.8 m represents a separate fourth group. It is also characterized by a bimodal distribution with two peaks close in values: coarse silt (40%) and fine silt (31%). Medium silt also has a relatively high percentage (15%). Additionally, the amount of clay in the sample is the highest throughout the core and reaches 10%.

The fifth group is represented by a single sample in the interval 0.2–0.3 m. Its characteristics are close to the second group, with a predominance of fine sand (83%) suggesting a high-energy environment. However, this layer contains higher percentages of coarse and medium sand. These particles reach 16% in the sample, while clays and fine silt are practically absent (0.2 and 0.6%, respectively).

3.2. Geochemical Analysis

Geochemical compositions of analyzed sediments show the predominance of silica (Si), iron (Fe), and calcium (Ca) (Figure 2, Table 1). The high concentration of Ca (~28%) corresponds to the upper part of the core and could be related to shell fragments in the sediments. The high value of Fe corresponds to silt and clay fractions (>80%). The concentration of Ca and Sr are related to decreasing Fe, Si, and Ti values. The lower part of the core mainly consists of fine sand, with a high concentration of Si corresponding to the sand fraction.

Table 1. Rybachya core geochemical analysis results.

Depth (m)	Si (%)	Ti (%)	Fe (%)	Ca (%)	Sr (%)	Other Elements (%)
0.2–0.3	3.55	0.23	1.10	4.80	0.10	90.23
0.3–0.8	1.90	0.20	3.76	3.40	0.04	90.70
1.73–1.96	5.30	0.31	1.37	3.14	0.03	89.85
2.15–2.20	4.30	0.24	1.53	3.25	0.02	90.65
2.35–2.34	3.06	0.26	3.31	3.68	0.03	89.66
3.13–3.50	0.95	0.00	0.69	28.20	0.29	69.87
4.25–4.40	4.28	0.10	0.98	1.01	0.01	93.62
6.3–6.4	6.57	0.12	0.93	1.03	0.01	91.33
9.40–9.50	5.61	0.16	1.12	1.58	0.01	91.52

3.3. Mollusk Fauna

The mollusk fauna in the core contains 16 species (Figures 3 and 4). These taxa have different ecologies and are adapted for basins with different hydrological and hydrochemical regimes. The biostratigraphic index fossil *Didacna* Eichwald is absent.

Samples from the lower sandy unit (below 3.7 m) do not contain mollusk shells. Only a single indeterminate fragment was found.

Assemblage I: The sediments of the overlying unit (3.50–3.13 m) are dominated by *Theodoxus pallasi* (Lindholm, 1924), rare *Dreissena polymorpha*, and *Lymnaea stagnalis* (Linnaeus, 1758).

Assemblage II: The 2.34–2.25 m interval contains abundant *Monodacna caspia* and *Dreissena polymorpha*, along with *Dreissena caspia* (Eichwald, 1855), *Clessiniola variabilis* (Eichwald, 1838), *Unio* sp. (small fragments), *Viviparus* sp. (debris), and *Valvata piscinalis* (O. F. Müller, 1774). The interval of 2.27–2.23 m contains very rare shells of *Bithynia tentaculata* (Linnaeus, 1758), *Clessiniola variabilis*, and small fragments of *Unio* shells. At 2.20–2.16 m, shell material is rare, and it contains *Monodacna caspia*, *Clessiniola variabilis*, *Dreissena polymorpha*, small fragments of *Unio* sp., and *Planorbis* sp. As well. The sample from the interval 2.22–2.14 m includes abundant specimens of *Dreissena polymorpha*, rare *Clessiniola variabilis*, *Lymnaea stagnalis*, *Monodacna caspia*, and a single fragment of *Valvata* sp. The next interval at the depths of 2.11–2.07 m includes infrequent, well-preserved shell fragments of *Dreissena polymorpha*, *Hypanis plicata*, *Valvata piscinalis*, *Clessiniola variabilis*, *Unio* sp., *Valvata* sp., and *Planorbis* sp. The interval 1.96–1.73 m is characterized by *Viviparus viviparus* (Linnaeus, 1758), *Valvata piscinalis*, *Planorbis planorbis* (Linnaeus, 1758), *Unio* sp. (fragment), *Dreissena polymorpha*, *Dreissena caspia*, *Monodacna caspia*, *Clessiniola variabilis*, *Theodoxus pallasi*, and *Abeskunus brusinianus* (Clessin and W. Dybowski, 1887).

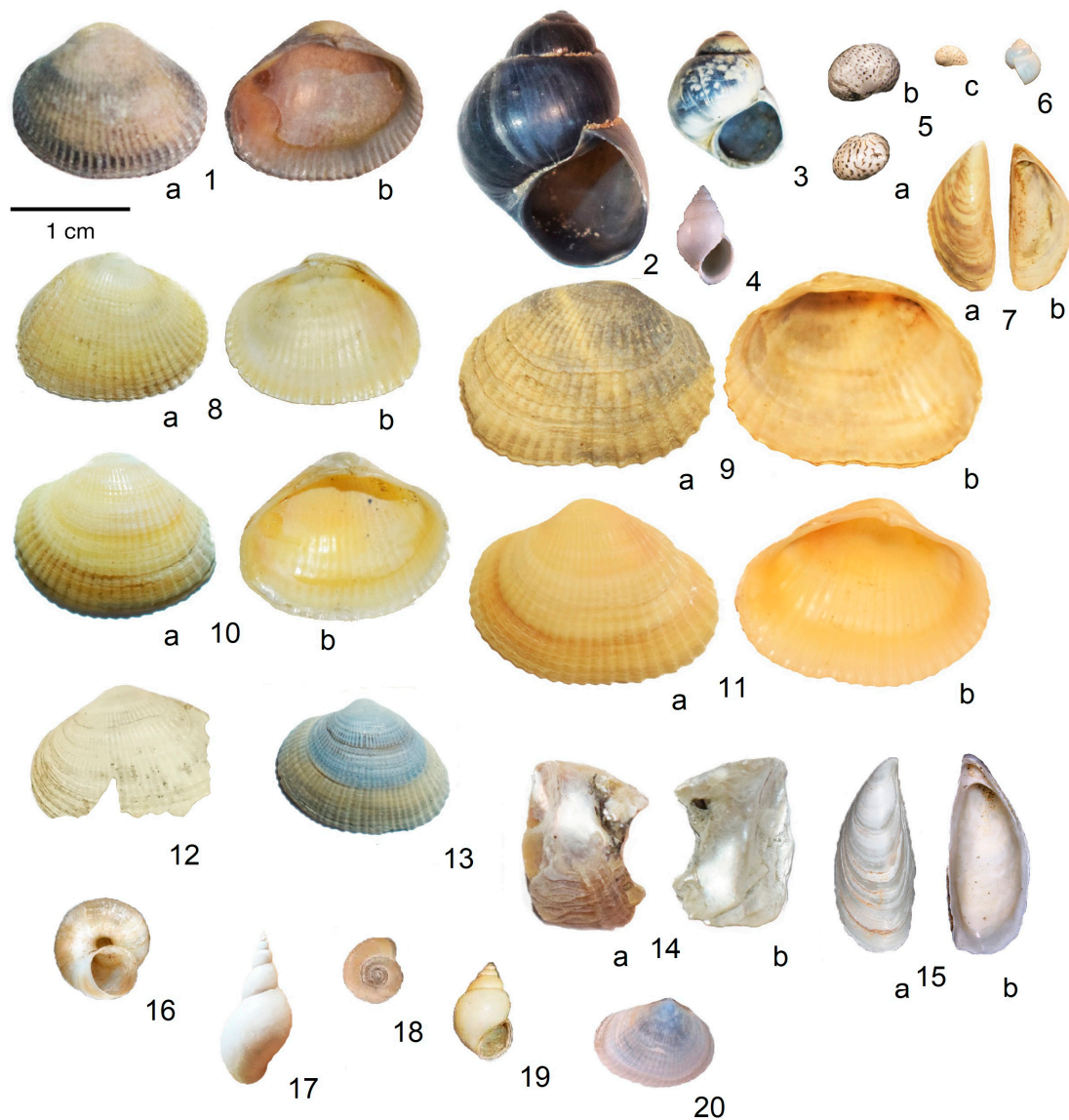


Figure 3. Mollusk fauna of the studied Rybachya core ((a) outer view, (b) internal view). (1), (8), (10), (13) *Monodacna caspia*; (2), (3) *Viviparus viviparus*; (4) *Clessiniola variabilis*; (5a, b, c) *Theodoxus pallasii*; (6) *Abeskunus brusinianus*; (7) *Dreissena polymorpha*; (9) *Hypanis plicata*; (11) *Monodacna angusticostata*; (12) *Didacna* sp.; (14) *Unio* sp.; (15) *Dreissena caspia*; (16) *Valvata piscinalis*; (17) *Lymnea stagnalis*; (18) *Planorbis planorbis*; (19) *Bithynia tentaculata*; (20) *Adacna vitrea*. Scale bars 1 cm.

Assemblage III: The interval 0.80–0.30 m contains only detritus, while samples from the core upper part (0.30–0.20 m) interval contain a prevalence of *Monodacna caspia*, numerous *Monodacna angusticostata* (Borcea, 1926), and *Dreissena caspia*, with rare specimens of *Hypanis plicata*, *Bithynia tentaculata*, *Theodoxus pallasii*, *Adacna vitrea* (Eichwald, 1829), *Clessiniola variabilis*, and small fragments of *Didacna* sp.

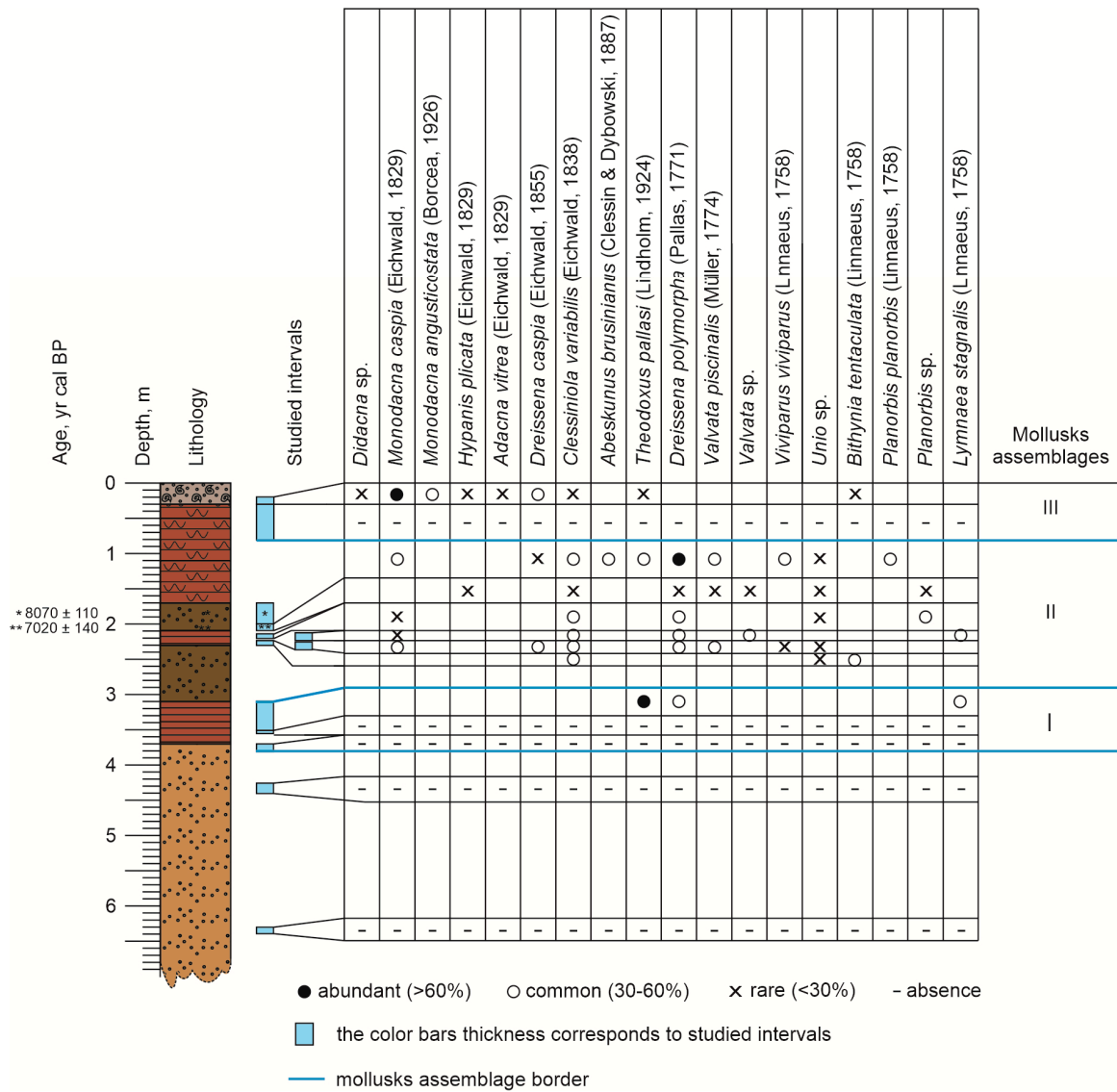


Figure 4. Rybachya core list of mollusks (grouped from left to right from marine/brackish water to freshwater species).

3.4. Diatoms

Ninety-five diatom species were distinguished that represent five diatom assemblages (or ecozones) (Figures 5 and 6). They were established using data on taxonomic diversity, dominant species, concentration of diatom valves (mln valves/g of air-dried sediment), and ecological characteristics of the species [43]. Reconstructed environments range from freshwater and shallow inter-distributary bays and channels to typical marine sedimentation. The samples vary greatly in the concentration of diatom valves along the core from 0.34 to 25.2 mln valves/g.

Assemblage I (3.8–3.9 m) was established within the silty sand layer by single valves of the following freshwater diatoms: *Fragilaria capucina* (Desmazières, 1830), *Aulacoseira granulata* (Ehrenberg) Simonsen, 1979, and *Cocconeis placentula* (Ehrenberg, 1838). The amount of diatom valves found in the interval does not supply correct calculations of the concentration of diatom valves.

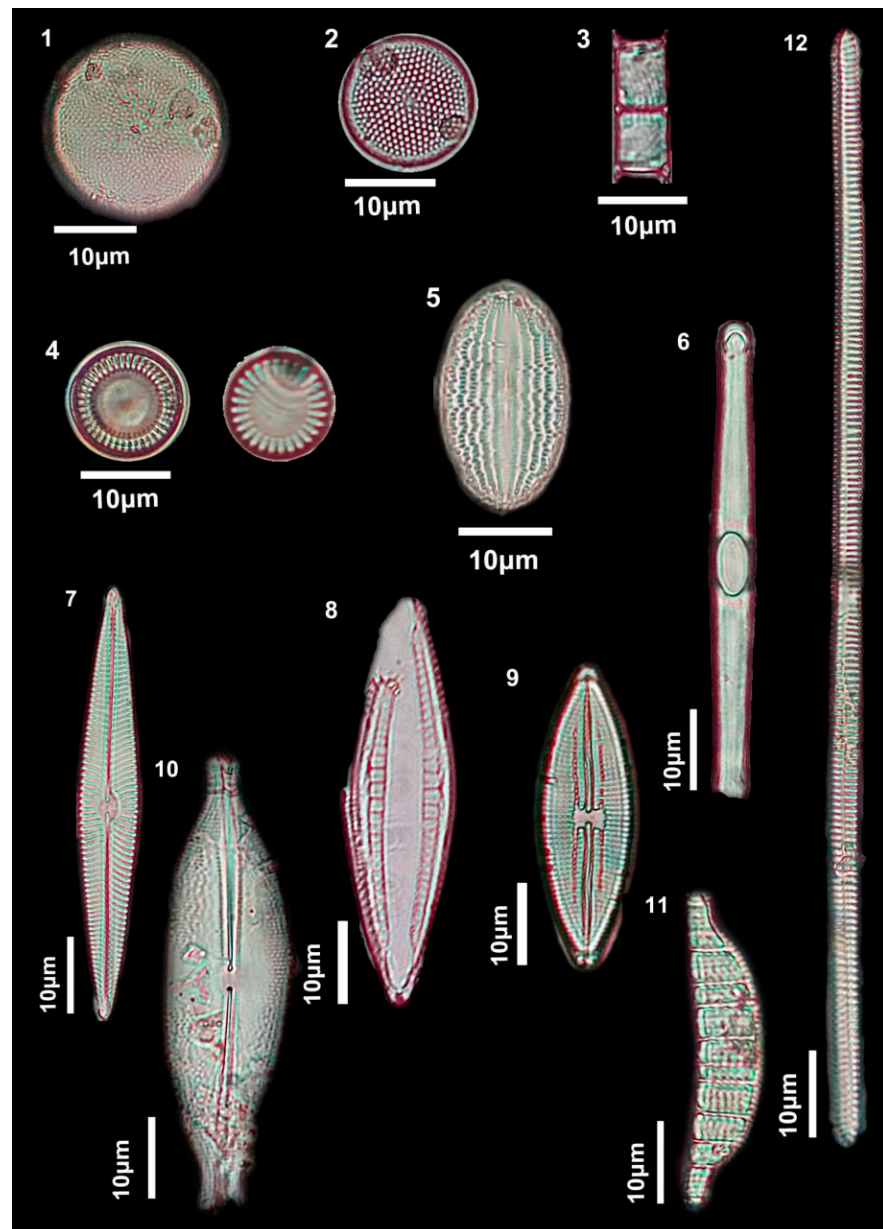


Figure 5. Diatoms of the studied Rybachya core. (1) *Actinocyclus octonarius*; (2) *Thalassiosira eccentrica* (Ehrenberg) Cleve, 1904; (3) *Aulacoseira italica* (Ehrenberg) Simonsen, 1979; (4) *Stephanocyclus meneghinianus*; (5) *Cocconeis lineata*; (6) *Grammatophora macilentata*; (7) *Navicula avenacea*; (8) *Mastogloia pseudexigua*; (9) *Lyrella lyra*; (10) *Anomoeoneis sphaerophora* (Pfitzer, 1871); (11) *Epithemia adnata* (Kützing) Brébisson, 1838; (12) *Ulnaria ulna* (Nitzsch) Compère, 2001.

Assemblage II (3.5–3.0 m) occurred within sapropels with plant remains. It was established by a high abundance of benthic diatoms (up to 100%) and a rather high concentration of diatom valves, which increases upwards from 1.8 to 13.2 mln valves/g (Figure 6). The periphyton species of the genus *Epithemia* dominate (70%). Subordinate species are brackish water *Navicula libonensis* (Schoeman, 1970) and *Mastogloia pseudexigua* (Cholnoky, 1956) (Figure 5). In the diatom assemblage, poor preservation of the valves and an increasing abundance of alkaliphilous and alkalibiontic diatoms was noted.

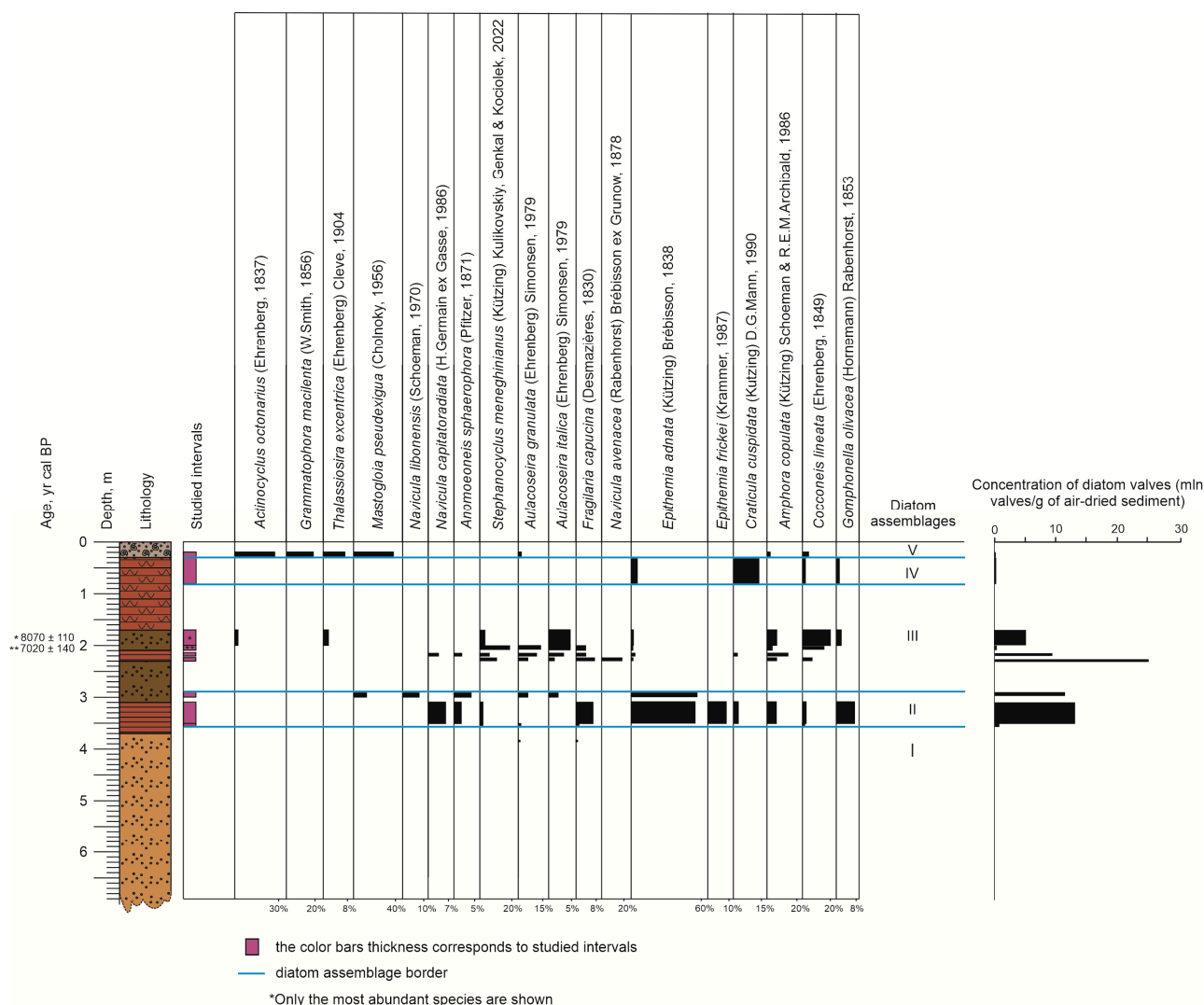


Figure 6. Rybachya core list of diatoms (grouped from left to right from marine/brackish water to freshwater species).

Assemblage III (2.4–1.7 m) was distinguished in clay sediments coarsening-upward and is characterized by different dominant species and the highest average valve abundance, which varied from 1.0 to 25.2 mln valves/g. The maxima of the valve concentration is at the depth of 2.2–2.4 m. The predominant freshwater taxa point to environments of lower delta: *Stephanocyclus meneghinianus* (Kützing) Kulikovskiy, Genkal and Kociolek, 2022, *Cocconeis lineata* (Ehrenberg, 1849). A relatively high abundance of benthic brackish water species *Navicula avenacea* (Rabenhorst) Brébisson ex Grunow, 1878 (19%) was observed.

Assemblage IV (0.8–0.3 m) was identified in sapropels and characterized by the abundant benthic freshwater species *Lyrella lyra* (Ehrenberg) Karayeva, 1978 (44%), found only in this interval. Subordinates are alkaliphilous benthic species *Craticula cuspidata* (Kützing) D.G.Mann, 1990 (14%), and mesohalobus planktonic *Amphora commutata* (Grunow, 1880) (7%). The concentration of diatom valves decreased to 0.8 mln valves/g.

Assemblage V (0.3–0.2 m) occurred in the sandy debris layer. It was established by a rather high content of the following planktonic marine diatoms: *Actinocyclus octonarius* (Ehrenberg, 1837) (30%) and its variety *A. octonarius var. tenellus* (Brébisson) Hendey, 1954 (4%), typical for the Caspian Sea and mesohalobus benthic species *Grammatophora macilenta* (W.Smith, 1856) (17%). The interval is characterized by the lowest concentration of diatom valves (0.3 mln valves/g). In total, a high abundance of planktonic diatoms (56%) was noted.

3.5. Ostracods

Twenty-three ostracod species were recorded in the samples taken from the Rybachya core (Figures 7–9).

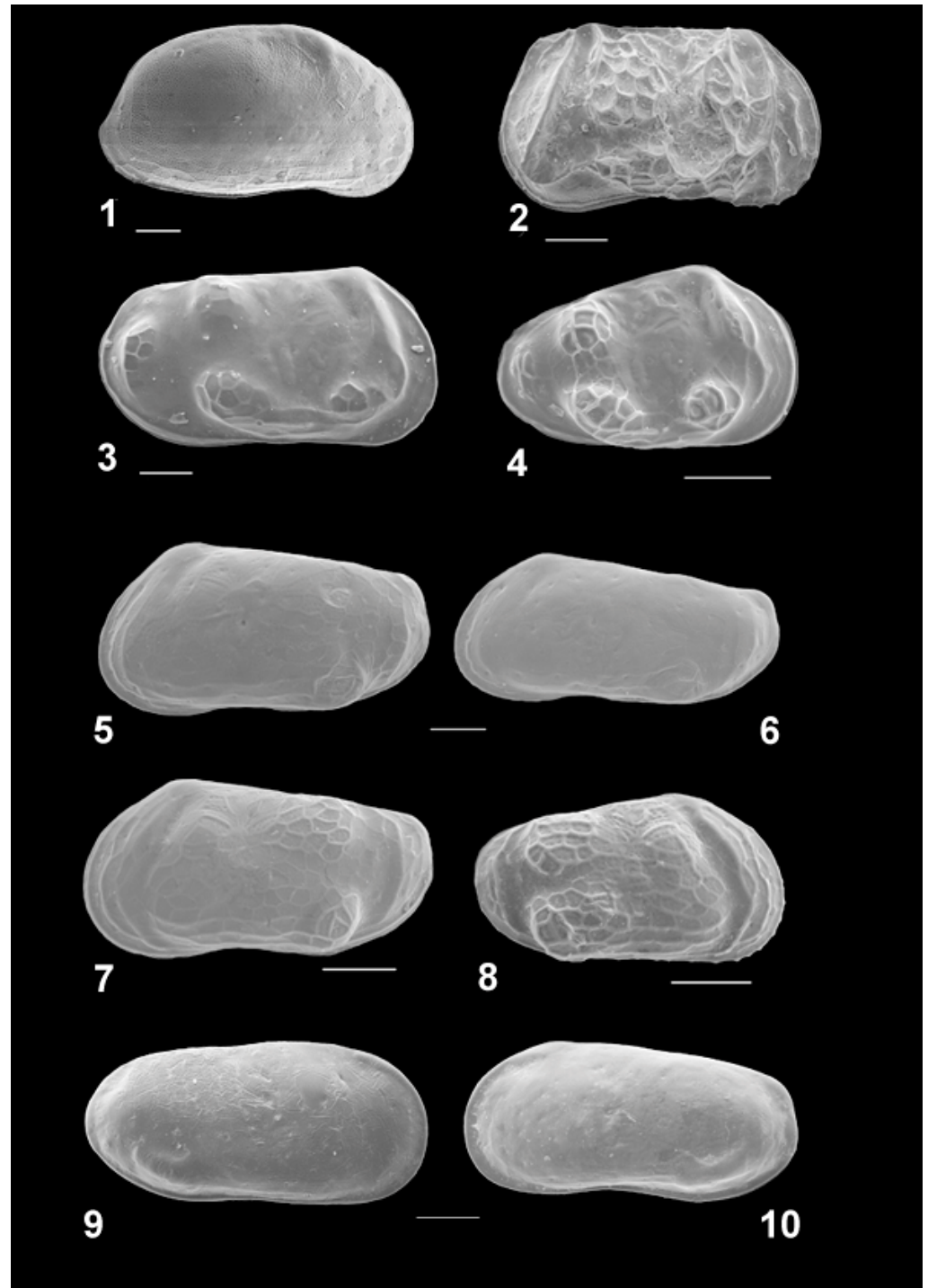


Figure 7. Ostracods of the studied Rybachya core. RV, right valve; LV, left valve; f, female; m, male; Ad, adult stages; juv, juvenile stages. Scale bar 100 μm . (1) *Tyrrhenocythere amnicola donetziensis*, RvAd; (2) *Euxinocythere baquana*, RVf; (3)–(4) *Amnicythere? quinquetuberculata*, RVAd and RVjuv; (5)–(8) *Amnicythere longa*, LVf, LVm, LVA-1, and RVA-3; (9)–(10) *Amnicythere cymbula*, RVf and LVm.

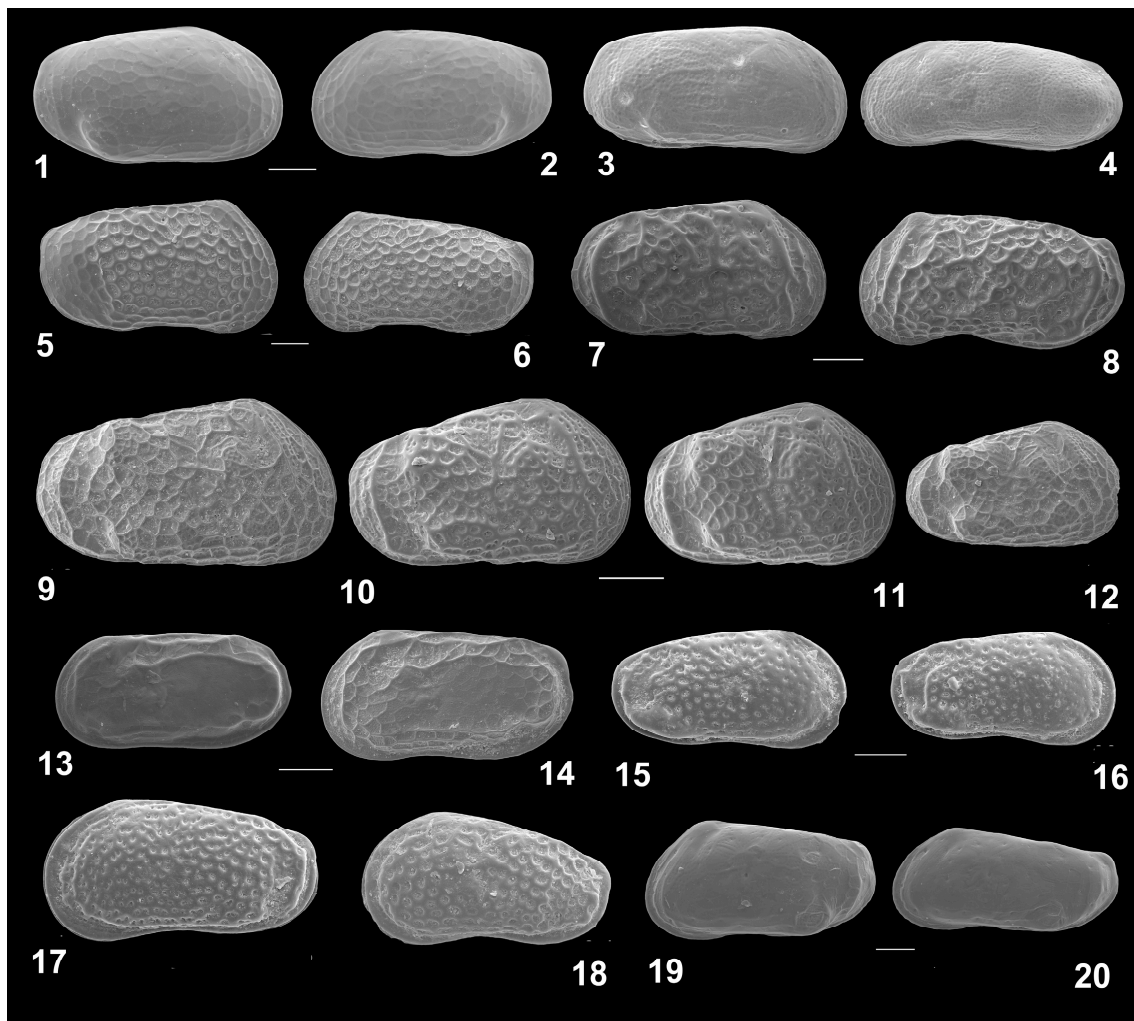


Figure 8. Ostracods of the studied Rybachya core. RV, right valve; LV, left valve; f, female; m, male; Ad, adult stages; juv, juvenile stages. Scale bar 100 μm . (1)–(2) *Amnicythere pirsagatica* (Livental in Agalarova et al., 1940), RVf and LVf; (3)–(4) *Amnicythere reticulata* (Schornikov, 1966), RVf and LVm; (5)–(6) *Amnicythere martha* (Livental in Agalarova et al., 1940), RVf и LVm; (7)–(12) *Euxinocythere bosqueti*, RVf and LVm, RVjv (9–12); (13)–(14) *Amnicythere caspia* (Livental, 1938), LVm and LVf; (15)–(18) *Euxinocythere relictata* (Schornikov, 1964), RVf, RVf, LVf, LVA–1; (19)–(20) *Amnicythere longa*, LVf and LVm.

These species form two groups based on their habitat preference type: the freshwater/oligohaline (4 taxa) and the Caspian (19 taxa) types. Depending on variation in the habitat type and salinity tolerance, the core was subdivided into four intervals characterized by the different assemblages. Assemblage I corresponded to the 6.3–6.4 m interval and was dominated by *Cyprideis torosa* (Jones, 1850) and *Tyrrhenocythere amnicola donetziensis* (Dubowsky, 1926), and it was most similar to the modern Caspian marine environment. No traces of redeposition were noted.

Assemblage II was identified in the interval of 3.0–3.5 m and was characterized by a high content of freshwater ostracod species (only two brackish water species are found). Abundant *C. torosa*, *T. amnicola donetziensis*, *Darwinula stevensoni* (Brady et Robertson, 1870), and *Candoninae* spp. were identified. All species encountered were adapted to live in shallow, freshwater basins, in waters tolerant of a wide temperature range.

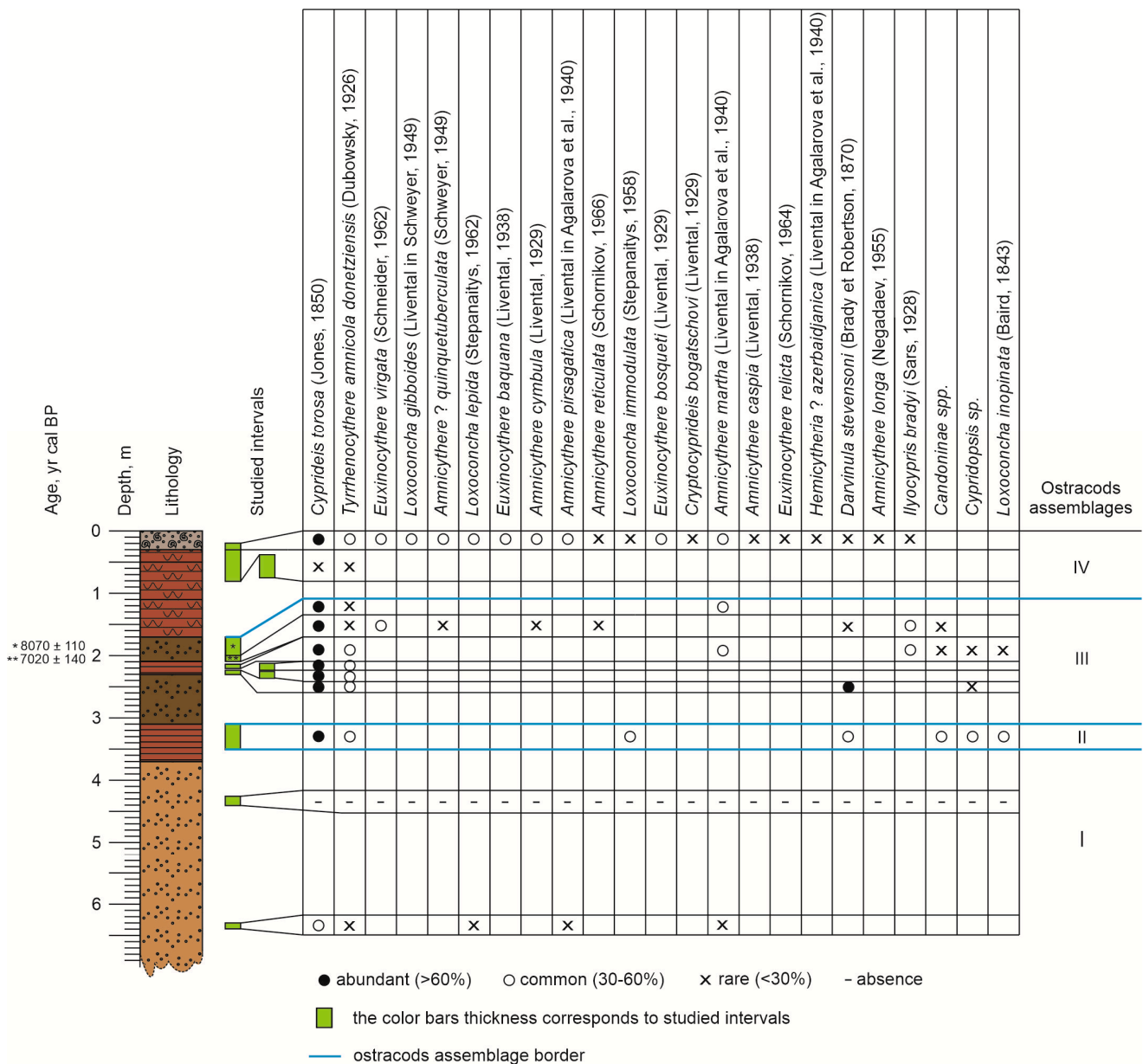


Figure 9. Rybachya core list of ostracods (grouped from left to right from marine/brackish water to freshwater species).

Assemblage III was observed at a depth of 1.73–2.5 m and generally can be described as brackish water with an admixture of freshwater species. *C. torosa* and *T. amnicola donetziensis* are abundant, with subordinates *Ilyocypris bradyi* (Sars, 1928) and *D. stevensoni*.

Assemblage IV was restricted to core-top sediments. Interval 0.2–0.3 m contained modern microfauna typical for the North Caspian dominated by *C. torosa*, *T. amnicola donetziensis*, more stenogaline *Cryptocyprideis bogatschovi* (Livental, 1929) (12.5–13.25‰), *Euxinocythere baquana* (Livental, 1938) (11.5–13‰), and *Amnicythere? quinquetuberculata* (Schweyer, 1949) (11.5–13‰) [55]. Rare *I. bradyi*, *D. stevensoni* or *Amnicythere longa* (Negadaev, 1955) and *Amnicythere cymbula* (Livental, 1929) were identified.

3.6. Radiocarbon Dating

Both samples were within a measurable range and yielded ¹⁴C ages of 7240 ± 110 yr in the 1.73–1.96 m interval and 6140 ± 110 yr in the 2.07–2.11 m interval. Calibrated with

the “IntCal 20” curve, the calculated ages were 8070 ± 110 cal yr BP and 7020 ± 140 cal yr BP, respectively.

4. Discussion

Among various scale paleogeographic events recorded in the Northern Caspian sediments during the Holocene, two epochs are particularly notable—the Mangyshlak regression and the Neocaspian transgression subdivided into several stages [32]. Relatively high heat supply and aridity [56] initiated a regressive trend in the Caspian Sea during the early Holocene. Pollen analyses showed an increase in xerophytes in the regional vegetation [57,58]. Beyond that, the Mangyshlak epoch included a climatic episode known as the «8200 event»—a brief significant cooling [59] reflected in increased aridity and the Caspian Sea retreat. Such climate conditions created a favorable environment for erosion in a drained area and the formation of paleovalleys. Usually, the thickness of Holocene deposits does not exceed 2 m within the study area [1,14,16,20,25,30–32]. Additionally, our mollusk, diatom, and ostracod data allowed us to reconstruct environmental conditions not typical for the marine shelf. This has led to the assumption that the Rybachya core was located within a paleovalley widespread in the North Caspian, as proposed by Bezrodnykh Y.P. and Sorokin V.M. [19]. The Mangyshlak regression left traces observable in seismogram signals, such as incised river valleys and numerous sublatitudinal linear depressions, resembling shallow lake basins (or “ilmens”) occurring in the Volga delta nowadays [32]. The interpretation of seismic data revealed that Mangyshlak deposits fill paleovalleys in the strata of the Khvalynian deposits in the same way as recorded in the Rybachya core reported in this article.

We compared the assemblages and identified four units based on the multi-proxy analysis of the Rybachya core samples. Each unit included assemblages with a similar ecology and sedimentation environment (Figure 10). Basal unit included (I) assemblage of ostracods and (I) assemblage of diatoms. Unit 1 included (I) mollusk assemblage, (II) ostracod assemblage, and (II) diatoms assemblage. Unit 2 included (II) mollusk assemblage, (III) ostracods assemblage, and (III) diatom assemblage. Unit 3 included (III) mollusk assemblage, (IV) ostracod assemblage, and (IV–V) diatom assemblages.

The leading geochemical indicators for identifying and correlating Caspian marine deposits with regional stratigraphy are the records of Fe, Al, Si, and Ti concentrations in the profile [60]. The primary sources of terrigenous material for the North Caspian are Pleistocene moraines, rich in Fe and Al, located in the upper reaches of the Volga basin [61,62]. High Fe, Al, and Ti concentrations usually correspond to lower Khvalynian deposits, especially in clay and silt sediments [60,63]. The comparative analysis of Fe concentration with grain size also supported it. The high Fe values correspond to silt and clay fractions. High concentrations of Ca and Sr are related to decreasing Fe, Si, and Ti values and potentially indicate a relative stabilization and salinity rise of the Caspian basins during the early Khvalynian stage. The lower part of the core mainly consists of fine sand with a high concentration of Si, which could be related to deltaic and upper shoreface facies during the transgression stage of the early Khvalynian basin. The Rybachya core from the early Khvalynian deposits had no traces of redeposition. Results of the geochemical analyses imply that the lower sandy (basal) unit (Figure 10), accumulated during the transgressive stage in deltaic or upper shoreface settings, is rich in Si, and geochemical markers confirmed the early Khvalynian age. Cumulative and particle size distribution curves practically coincide for the basal unit samples, which means they were deposited in similar high-energy environments with an additional source of fine silt. The absence of mollusk shells confirms the high-hydrodynamic depositional environment. A low concentration of diatoms resulted from a high sedimentation rate, preventing the formation of taphocoenosis. The ostracod assemblage points to a deeper basin with lower salinity than the modern Caspian Sea. It leaves no doubt about the early Khvalynian age of the lower core unit. The preservation of ostracods *Limnocythere inopinata* (Baird, 1843) is related to a high sedimentation rate, high mortality rate, or good preservation in deep waters [64].

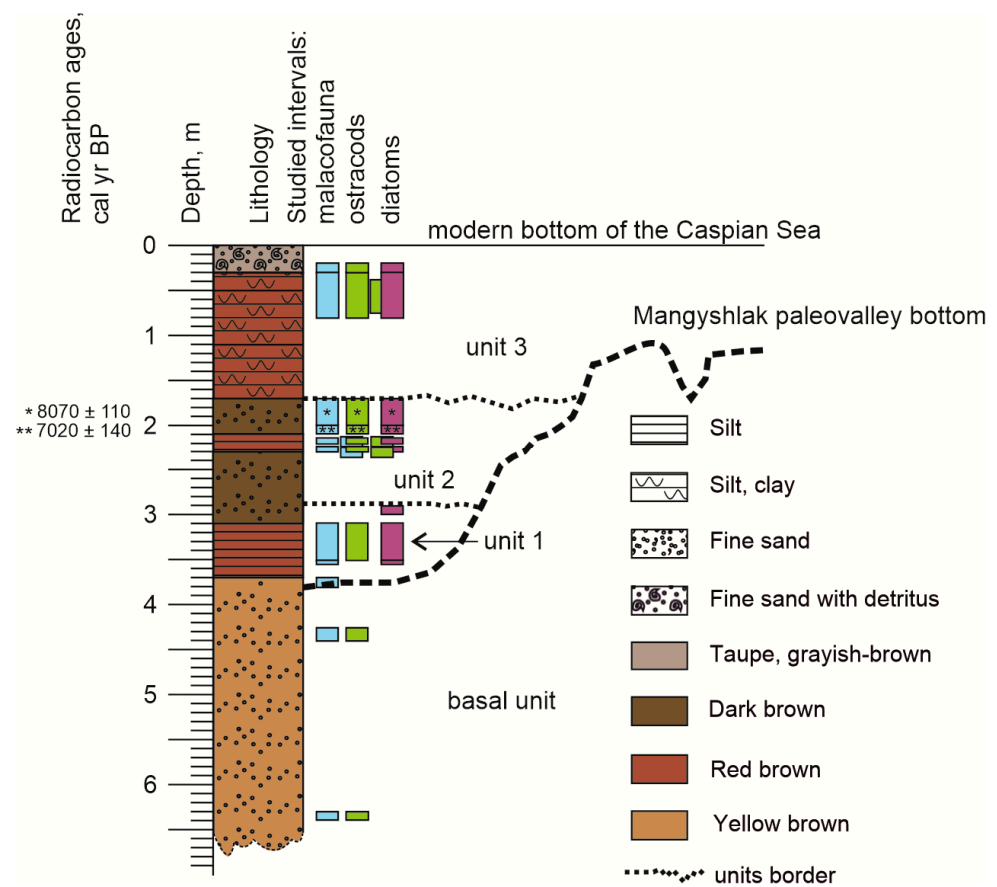


Figure 10. Evolutionary scheme of the Rybachya site. The color bars thickness corresponds to study intervals (blue for mollusk fauna, purple for diatoms, green for ostracods). Paleovalley structure shown after [19,32].

The Mangyshlak flow formed the paleovalley inferred from the Rybachya core and eroded the late Khvalynian deposits, although we do not see traces of it in the core structure. Lack of fauna at the base of the paleovalley is a consequence of erosion paleoevents, while rare valves of freshwater diatoms (*Fragilaria capucina*, *Aulacoseira granulata* and *Cocconeis placentula*) are remnants of the freshwater community in the channel during the downcutting erosion.

Based on the radiocarbon data, there are three Holocene stages of paleovalley repletion corresponding to the three units described below. Mollusk fauna, ostracods, and diatom species diversity is the result of evolutionary processes during the Pleistocene that occurred as a response to climatic changes and the transgressive-regressive rhythm of the Caspian Sea. Specimen abundance and faunal composition do not suggest stable environmental conditions during the deposition of these sediments. The biological proxies indicate quasi-cyclic variability throughout the core.

Increased concentrations of Ca and Sr in the first unit (Figures 2 and 10) indicate the rise of salinity and temperature in the Caspian basin, and together with a decrease of Fe and Ti values, it may denote the ingression of Caspian waters along the Mangyshlak depression and possibly mark the Neocaspian onset. It is estimated that the Neocaspian transgression started at 10,550 cal yr BP in the North Caspian [16], while for the southeastern Iranian coast of the Caspian Sea [65] and for the Middle and Southern Caspian [66], it started at 9500 cal yr BP [19] and was not older than 10,000 cal yr BP [30] and 8900 cal yr BP respectively [32]. The sea-level rise was followed by a sea-level drop and paleovalley isolation. Freshwater mollusk fauna, dominated by *Theodoxus pallasii*—native species—[67,68], *Dreissena polymorpha*, and *Lymnaea stagnalis*, comprised the first unit (Figure 10) from the paleovalley bottom to the depth of 3 m. The habitat of *D. polymorpha* was restricted

to the freshwater Volga delta and adjacent rivers [69]. *Lymnaea stagnalis* is a typical lake species. The presence of mollusk species adapted to living in the desalinated Caspian waters, and a high abundance of benthic and freshwater diatoms and freshwater and euryhaline ostracod species (*D. stevensoni*, *C. torosa*) assume a desalinated impound basin and lake-like environment during the initial sedimentation stage in the paleovalley. The high abundance of ostracod *C. torosa* is potentially linked to the abundant supply of organic matter and the high local productivity of the region as well. *C. torosa* reaches the maximum abundance because of highly variable salinity conditions at the time. Smith A.J. and Horne J.H. [70] indicated such a state as the transition from marine to freshwater conditions. *D. stevensoni* tolerates low salinity [71]. Modern forms of *Candoninae* spp. are considered inhabitants of desalinated water bodies. Grain size confirms backwater conditions, with deposits from the first unit formed in a more stagnant water environment than the sediments of the basal unit. Diatom concentration increases significantly, which is assumed to result from an increased nutrient river runoff. Based on our data, we assume that the sea retreat and isolation of the paleovalley accompanied the process of filling the depression with fresh waters. Following the transition from the marine to the freshwater conditions indicated by faunal remains, the tranquil waters of the small perennial basin contributed to the predominant accumulation of silt and clay. Similar results were reported for a site in the North Caspian Sea near the Rybachya core [16], where comparable sediments formed in shallower and more freshwater conditions than modern ones.

The second unit (Figure 10), identified at 3.0–1.73 m core depths, recorded the Caspian Sea-level rise. Radiocarbon data around 8–7 cal kyr BP determined the age of the accumulated sediments as the early Neocaspian, since the end of the first impulse of sea-level rise was dated as 5600 cal yr BP [32]. Grain size data show the interbedding of silty deposits in the interval of 2.2–2.3 m, formed in a more stagnant water environment, and fine sand, at a depth of 2.1–2.2 m and 1.7–2.0 m, corresponding to a transitional sedimentary environment from a tranquil water regime to a more dynamic one.

The mollusk assemblage contains abundant brackish water *Monodacna caspia*, *Dreissena caspia*, *Clessiniola variabilis*, *Hypanis plicata*, and *Abeskunus brusinianus* and freshwater *Dreissena polymorpha*, *Lymnaea stagnalis*, *Abeskunus brusinianus*, *Unio* sp., *Viviparus* sp., *Planorbis* sp., and *Valvata piscinalis* [13,25,37,68]. Silty deposits contain rare *Bithynia tentaculata*, *Clessiniola variabilis*, and small fragments of *Unio* shells. The upper salinity tolerance of *M. caspia* was previously reported as 8‰ [72], but recently [73], this species was found in the middle and southern Caspian Sea, and its salinity tolerance was extended to 12–13‰. The presence of brackish water ostracods with an admixture of freshwater species (*I. bradyi*, *D. stevensoni*) and a relatively high abundance of benthic brackish water diatom species *Navicula avenacea* provide evidence of complex internal hydrodynamics during the transgressive stage. Dynamic changes occurred in the area [16], where shelf flooding due to sea-level rise at the beginning of the Neocaspian time was followed by fluctuations from marine to freshwater and, later, brackish water conditions and eventually the formation of a stagnant basin.

We interpreted the observed freshwater communities found in silty sediments with high values of Fe and Ti as the late Khvalynian. In the Northern Caspian Lowland [74], these communities can be found in the redeposited late Khvalynian sediments eroded at the paleovalley area but preserved in surrounding areas. In this case, a high concentration of these elements at the base of the second unit might be related to erosion of the late Khvalynian sediments.

Our radiocarbon ages are younger than the previously published ones. In previous studies, ^{14}C data suggested the paleovalleys in the North Caspian to be filled between 11,500 and 8000 cal yr BP [32]. However, their paleoenvironment reconstruction confirms our interpretation. The depositional environment was freshwater or slightly brackish water, as demonstrated by the sedimentary sequence and fossil plant and faunal assemblages. Therefore, we assumed a later and longer sedimentation process started with extended warming and humidification, as proposed by Bolikhovskaya N.S. [57], from 8500 to 7600 yr BP for the Caspian Sea region. Warm and humid climatic conditions were reconstructed for

the East European Plain [75,76] for this period of higher sea-level stand [6,7]. Regressive stages of a smaller scale than the Mangyshlak stage (nk^2 and nk^4 when sea-level dropped by 5–6 m) were identified during the Neocaspian transgressive epoch; however, we could not find evidence of these in the Rybachya core, and therefore could not confirm or deny the erosion origin. Nevertheless, we assume changes in mollusk, ostracod, and diatom faunal assemblages observed in the current study are evidence of sea-level oscillations during the Neocaspian time dated as 5600–3700 cal yr BP and 3080–2300 cal yr BP [32].

The upper part of the third unit (Figure 10) corresponds to the modern Caspian Sea sedimentation. A sharp contact between the unit and the underlying layer was interpreted as a hiatus. Based on the diatom assemblage composition at the bottom of the unit, sedimentation took place in a freshened shallow marine bay or lagoon. The poor preservation of diatom valves and a relatively high abundance of alkaliphilous and mesohalobous diatoms indicate an alkaline environment. Elements such as Fe and Ti are assumed to be the main geochemical indicators for the identification and correlation of Caspian marine deposits on the regional stratigraphy level. These elements demonstrate high concentrations along the unit [60]. The mollusk assemblage is dominated by Caspian slightly brackish water taxa *Monodacna caspia*, *M. angusticostata*, *Dreissena caspia*, *Didacna* sp. etc., typical for the modern northern part of the Caspian Sea [13,77–80]. Ostracod assemblage indicates shallow water conditions and contains abundant euryhaline species tolerant to reduced salinities reflecting the Volga River influence in the area (*Amnicythere longa* and *Amnicythere cymbula* are common in estuaries in the Black Sea at depths up to 5 m [81] and show the extent of the Volga delta influence in this area). The increase in typical planktonic marine species in the diatom assemblage reflects the influence of sea-level rise and corresponds to the latest Caspian Sea transgressive stage following the regressive event after 2300 cal yr BP [32]. Likewise, the last sedimentation stage in the nearby area was described [16] as a fairly stable environment, similar to the modern in terms of water depth and salinity.

5. Conclusions

Paleoenvironmental evidence presented here based on mollusk, diatom, and ostracod fauna, geochemical, and grain size data allows us to conclude that the Rybachya core documents a widespread paleovalley environment in the North Caspian. The diversity of studied fossil groups contributes to the step-by-step paleoreconstruction of the Rybachya core. For the first time, a paleovalley filling sequence was established in the North Caspian region based on the multi-proxy analysis of the core. The core was obtained from the early Khvalynian deposits. The Mangyshlak flow formed the depression and eroded the late Khvalynian deposits, which we did not observe in the core structure. We distinguished three stages of paleovalley repletion in the overlying units according to radiocarbon data. Observed mollusk, ostracod, and diatom species diversity is the result of evolutionary processes during the Pleistocene that occurred in response to climatic changes and the transgressive-regressive rhythm of the Caspian Sea. The biological proxies indicate quasi-cyclic variability throughout the core. Lithologically, deposits from some of the units were formed under more stagnant hydrodynamic conditions at transgressive Neocaspian stages or an insulated freshwater basin during a regressive episode of the Neocaspian epoch. Such environmental conditions were interrupted by the transitional phase inherent in a higher-energy environment. Paleovalley gradual filling during the Holocene ended under marine conditions typical for the modern Caspian Sea.

Author Contributions: Conceptualization, A.B. and E.L.; formal analysis, A.B., E.L., R.M., M.Z. and T.Y.; investigation, A.B., E.L., R.M. and T.Y.; resources, T.Y.; data curation, A.B.; writing—original draft preparation, A.B.; writing—review and editing, A.B., E.L., R.M., M.Z. and T.Y.; visualization, A.B. and E.L.; supervision, T.Y.; project administration, T.Y.; funding acquisition, A.B., R.M. and T.Y. All authors have read and agreed to the published version of the manuscript.

Funding: This research was funded by Russian Science Foundation, grant number 21-44-04401 and by Russian Foundation for Basic Research, grant number 20-35-90020.

Institutional Review Board Statement: Not applicable.

Informed Consent Statement: Not applicable.

Data Availability Statement: Not applicable.

Acknowledgments: We thank LLC (limited liability company) «Morinzhgeologiya» for the core material, Daria Semikolennykh for help with fauna images, and Anna Stepanova for manuscript editing.

Conflicts of Interest: The authors declare no conflict of interest. The funders had no role in the design of the study; in the collection, analyses, or interpretation of data; in the writing of the manuscript; or in the decision to publish the results.

References

1. Yanina, T.A.; Bolikhovskaya, N.S.; Sorokin, V.M.; Berdnikova, A.A.; Tkach, N.T. Paleogeography of the Caspian Sea in the Late Pleistocene—Holocene. In *Actual Problems of the Pleistocene Paleogeography. Scientific Achievements of the School of Academician K.K. Markov*; Yanina, T.A., Bolikhovskaya, N.S., Polyakova, Y.I., Klyuvitkina, T.S., Kurbanov, R.N., Eds.; Faculty of Geography, Moscow State University: Moscow, Russia, 2020; pp. 317–365.
2. Zonn, I.S. *The Caspian Encyclopedia*; International Relations Publ.: Moscow, Russia, 2004; pp. 1–461.
3. Kostianoy, A.G.; Kosarev, A.N. *The Caspian Sea Environment*; Springer: Berlin/Heidelberg, Germany, 2005; pp. 1–268. [\[CrossRef\]](#)
4. Sidorchuk, A.Y.; Panin, A.V.; Borisova, O.K. Morphology of river channels and surface runoff in the Volga River basin (East European Plain) during the Late Glacial period. *Geomorphology*. **2009**, *113*, 137–157. [\[CrossRef\]](#)
5. Panin, A.V.; Sidorchuk, A.Y.; Ukraintsev, V.Y. The Contribution of Glacial Melt Water to Annual Runoff of River Volga in the Last Glacial Epoch. *Water Resour.* **2021**, *48*, 877–885. [\[CrossRef\]](#)
6. Varushchenko, S.I.; Varushchenko, A.N.; Klige, R.K. *Change of Regime of Caspian Sea and Drainless Water Bodies in Paleotime*; Nauka: Moscow, Russia, 1987; 239p.
7. Rychagov, G.I. Holocene oscillations of the Caspian Sea, and forecasts based on palaeogeographical reconstructions. *Quat. Int.* **1997**, *41/42*, 167–172. [\[CrossRef\]](#)
8. Kislov, A.V.; Toropov, P.M. East European river runoff and Black Sea and Caspian Sea level changes as simulated within the Paleoclimate modeling intercomparison project. *Quat. Int.* **2007**, *167–168*, 40–48. [\[CrossRef\]](#)
9. Svitoch, A.A. Khvalynian transgression of the Caspian Sea was not a result of water overflow from the Siberian Proglacial lakes, nor a prototype of the Noachian flood. *Quat. Int.* **2009**, *197*, 115–125. [\[CrossRef\]](#)
10. Kislov, A.; Panin, A.V.; Toropov, P. Current status and palaeostages of the Caspian Sea as a potential evaluation tool for climate model simulations. *Quat. Int.* **2014**, *345*, 48–55. [\[CrossRef\]](#)
11. Yanina, T.A. The Ponto–Caspian region: Environmental consequences of climate change during the Late Pleistocene. *Quat. Int.* **2014**, *345*, 88–99. [\[CrossRef\]](#)
12. Koriche, S.A.; Singarayer, J.S.; Cloke, H.L.; Valdes, P.J.; Wesselingh, F.P.; Kroonenberg, S.B.; Wickert, A.D.; Yanina, T.A. What are the drivers of Caspian Sea level variation during the late Quaternary? *Quat. Sci. Rev.* **2022**, *283*, 107457. [\[CrossRef\]](#)
13. Yanina, T.A. *Didacnas of the Ponto–Caspian*; Madzhenta Press: Moscow/Smolensk, Russia, 2005; pp. 1–300.
14. Yanina, T.A. *Neopleistocene of the Ponto–Caspian Region: Biostratigraphy, Paleogeography, Correlation*; Lomonosov Moscow State University, Geographical Faculty: Moscow, Russia, 2012; pp. 1–264.
15. Boomer, I.; von Grafenstein, U.; Guichard, F.; Bieda, S. Modern and Holocene sublittoral ostracod assemblages (Crustacea) from the Caspian Sea: A unique brackish, deep–water environment. *Palaeogeogr. Palaeoclimatol. Palaeoecol.* **2005**, *225*, 173–186. [\[CrossRef\]](#)
16. Chekhovskaya, M.P.; Zenina, M.A.; Matul, A.G.; Stepanova, A.Y.; Rakovski, A.Z. Reconstruction Environmental Changes in the North Caspian Sea Shelf During the Holocene by Ostracoda. *Oceanology* **2018**, *58*, 89–101. [\[CrossRef\]](#)
17. Leroy, S.A.G.; Lopez–Merino, L.; Kozina, N. Dinocyst records from deep cores reveal a reversed salinity gradient in the Caspian Sea at 8.5–4.0 cal ka BP. *Quat. Sci. Rev.* **2019**, *209*, 1–12. [\[CrossRef\]](#)
18. Svitoch, A.A. Hierarchy and chronology of the Holocene oscillations of the Caspian Sea level. In *Changes of the Natural Territorial Complexes in the Zones of Anthropogenic Impact*; Media–Press: Moscow, Russia, 2006; pp. 125–132.
19. Bezrodnykh, Y.P.; Sorokin, V.M. On the age of the Mangyshlak deposits of the northern Caspian Sea. *Quat. R.* **2016**, *85*, 245–254. [\[CrossRef\]](#)
20. Svitoch, A.A.; Yanina, T.A. *Quaternary Sediments of the Caspian Sea Coasts*; Rosselchozakademiya: Moscow, Russia, 1997; pp. 1–267.
21. Zastrozhnov, A.S.; Danukalova, G.A.; Shick, S.M.; van Kolfshoten, T. State of stratigraphic knowledge of Quaternary deposits in European Russia: Unresolved issues and challenges for further research. *Quat. Int.* **2018**, *478*, 1–26. [\[CrossRef\]](#)
22. Krijgsman, W.; Tesakov, A.; Yanina, T.; Lazarev, S.; Danukalova, G.; Van Baak, C.G.; Agustí, J.; Alçiçek, M.C.; Aliyeva, E.; Bista, D.; et al. Quaternary time scales for the Pontocaspian domain: Interbasinal connectivity and faunal evolution. *Earth Sci. Rev.* **2019**, *188*, 1–40. [\[CrossRef\]](#)
23. Kroonenberg, S.B.; Abdurakhmanov, G.M.; Badyukova, E.V.; Van der Borg, K.; Kalashnikov, A.; Kasimov, N.S.; Rychagov, G.I.; Svitoch, A.A.; Vonhof, H.B.; Wesselingh, F.P. Solar–forced 2600 BP and Little ice age highstands of the Caspian sea. *Quat. Int.* **2007**, *173–174*, 137–143. [\[CrossRef\]](#)

24. Richards, K.; Mudie, P.; Rochon, A.; Athersuch, J.; Bolikhovskaya, N.; Hoogendoorn, R.; Verlinden, V. Late Pleistocene to Holocene evolution of the Emba delta, Kazakhstan, and coastline of the north-eastern Caspian Sea: Sediment, ostracods, pollen and dinoflagellate cyst records. *Palaeogeogr. Palaeoclimatol. Palaeoecol.* **2017**, *468*, 427–452. [[CrossRef](#)]
25. Fedorov, P.V. *Stratigraphy of Quaternary Deposits and History of Development of the Caspian Sea*; Trudy of the Geological Institute of the Academy of Science, Nauka: Moscow, Russia, 1957; Volume 10, pp. 1–308.
26. Andrusov, N.I. Sketch about development of the Caspian Sea and its inhabitants. *Izv. Russ. Geogr. Soc.* **1888**, *2*, 91–114.
27. Eichwald, E. Faunae Caspii maris primitivae. *Bull. De La Société Impériale Des Nat. De Moscou* **1838**, *II*, 125–174.
28. Pravoslavlev, P.A. Caspian deposits of the Ural River. *Izv. Don. Polytechn. Inst.* **1913**, *2*, 1–60.
29. Bogachev, V.V. Geological observations in the Manych valley, made in the summer of 1903. *Izv. Geol. Komissii* **1903**, *22*, 73–162.
30. Bezrodnykh, Y.P.; Romanyuk, B.F.; Deliya, S.V.; Magomedov, R.D.; Sorokin, V.M.; Parunin, O.B.; Babak, E.V. Biostratigraphy and structure of the Upper Quaternary deposits and some paleogeographic features of the north Caspian region. *Stratigr. Geol. Corr.* **2004**, *12*, 102–120.
31. Bezrodnykh, Y.P.; Deliya, S.V.; Romanyuk, B.F.; Sorokin, V.M.; Yanina, T.A. New data on the upper quaternary stratigraphy of the north Caspian sea. *Dokl. Earth Sci.* **2015**, *462*, 479–483. [[CrossRef](#)]
32. Bezrodnykh, Y.; Yanina, T.; Sorokin, V.; Romanyuk, B. The Northern Caspian Sea: Consequences of climate change for level fluctuations during the Holocene. *Quat. Int.* **2020**, *540*, 68–77. [[CrossRef](#)]
33. Rychagov, G.I. The sea-level regime of the Caspian Sea during the last 10,000 years. *Bull. Mosc. State Univ. Ser. 5* **1993**, *2*, 38–49.
34. Kachinskiy, N.A. *Soil Physics—Part 1*; Higher Education Publishing House (USSR): Moscow, Russia, 1965; pp. 1–324.
35. Rusakov, A.; Sedov, S. Late Quaternary pedogenesis in periglacial zone of northeastern Europe near ice margins since MIS 3: Timing, processes, and linkages to landscape evolution. *Quat. Int.* **2012**, *265*, 126–141. [[CrossRef](#)]
36. Lebedeva, M.; Makeev, A.; Rusakov, A.; Romanis, T.; Yanina, T.; Kurbanov, R.; Kust, P.; Varlamov, E. Landscape dynamics in the caspian lowlands since the last deglaciation reconstructed from the pedosedimentary sequence of srednaya Akhtuba, southern Russia. *Geosciences* **2018**, *8*, 492. [[CrossRef](#)]
37. Nevesskaja, L.A. History of the genus *Didacna* (Bivalvia: Cardiidae). *Paleontol. J.* **2007**, *41*, 861–949. [[CrossRef](#)]
38. Smol, J.P.; Birks, H.J.; Last, W.M. *Tracking Environmental Change Using Lake Sediments: Terrestrial, Algal and Siliceous Indicators*; Kluwer Academic Publishers: Alphen aan den Rijn, The Netherlands, 2001; pp. 1–327.
39. Krammer, K.; Lange-Bertalot, H. Bacillariophyceae. 1. Teil: Naviculaceae. In *Süßwasserflora von Mitteleuropa*; Ettl, H., Gerloff, J., Heynig, H., Mollenhauer, D., Eds.; Fisher Verlag: Jena, Germany, 1986; Volume 2, pp. 1–976.
40. Krammer, K.; Lange-Bertalot, H. Bacillariophyceae. 2. Teil: Bacillariaceae, Epithemiaceae, Surirellaceae. In *Süßwasserflora von Mitteleuropa*; Ettl, H., Gerloff, J., Heynig, H., Mollenhauer, D., Eds.; Fisher Verlag: Stuttgart, Germany, 1988; Volume 2, pp. 1–596.
41. Krammer, K.; Lange-Bertalot, H. Bacillariophyceae. 3. Teil: Centrales, Fragilariaceae, Eunotiaceae. In *Süßwasserflora von Mitteleuropa*; Ettl, H., Gerloff, J., Heynig, H., Mollenhauer, D., Eds.; Fisher Verlag: Jena, Germany, 1991; Volume 2, pp. 1–576.
42. Krammer, K.; Lange-Bertalot, H. Bacillariophyceae. 4. Teil: Achnantheaceae. Kritische Ergänzungen zu Navicula (Lineolatae) und Gomphonema. In *Süßwasserflora von Mitteleuropa*; Ettl, H., Gerloff, J., Heynig, H., Mollenhauer, D., Eds.; Fisher Verlag: Jena, Germany, 1991; Volume 2, pp. 1–437.
43. Zabelina, M.M.; Kiselev, I.A.; Proshkina-Lavrenko, A.I.; Sheshukova, V.S. *Key to the Freshwater Algae of the USSR. Iss. 4. Diatoms*; Nauka: Moscow, Russia, 1951; pp. 1–619.
44. Ivanova, E.V.; Marret, F.; Zenina, M.A.; Murdmaa, I.O.; Chepalyga, A.L.; Bradley, L.R.; Schornikov, E.I.; Levchenko, O.V.; Zyryanova, M.I. The Holocene Black Sea reconnection to the Mediterranean Sea: New insights from the northeastern Caucasian shelf. *Palaeogeogr. Palaeoclim. Palaeoecol.* **2015**, *427*, 41–61. [[CrossRef](#)]
45. Zenina, M.A.; Ivanova, E.V.; Bradley, L.R.; Murdmaa, I.O.; Schornikov, E.I.; Marret, F. Origin, migration pathways, and paleoenvironmental significance of Holocene ostracod records from the northeastern Black Sea shelf. *Quat. Res.* **2017**, *87*, 49–65. [[CrossRef](#)]
46. Zastrozhnov, A.; Danukalova, G.; Golovachev, M.; Osipova, E.; Kurmanov, R.; Zenina, M.; Zastrozhnov, D.; Kovalchuk, O.; Yakovlev, A.; Titov, V.; et al. Pleistocene palaeoenvironments in the Lower Volga region (Russia): Insights from a comprehensive biostratigraphical study of the Seroglazovka locality. *Quat. Int.* **2021**, *590*, 85–121. [[CrossRef](#)]
47. Agalarova, D.A.; Kadyrova, Z.K.; Kulieva, S.A. *Ostracoda from Pliocene and Post-Pliocene Deposits of Azerbaijan*; Azerbaijan State: Baku, Azerbaijan, 1961; pp. 1–419.
48. Mandelstam, M.I.; Markova, L.; Rosyeva, T.; Stepanaitys, N. *Ostracoda of the Pliocene and Post-Pliocene Deposits of Turkmenistan*; Turkmenistan Geological Institute: Ashkhabad, Turkmenistan, 1962; pp. 1–288.
49. Karmishina, G.I. *Pliocene Ostracoda from the Southern European Part of the USSR*; Izdatelstvo Saratovskogo Universiteta: Saratov, Russia, 1975; pp. 1–376.
50. Arslanov, K.A.; Tertychnaya, T.V.; Chernov, S.B. Problems and methods of dating low-activity samples by liquid scintillation counting. *Radiocarbon* **1993**, *35*, 393–398. [[CrossRef](#)]
51. Bronk Ramsey, C. Radiocarbon calibration and analysis of stratigraphy: The OxCal program. *Radiocarbon* **1995**, *37*, 425–430. [[CrossRef](#)]
52. Reimer, P.J.; Austin, W.E.; Bard, E.; Bayliss, A.; Blackwell, P.G.; Ramsey, C.B.; Butzin, M.; Cheng, H.; Edwards, R.L.; Friedrich, M.; et al. The IntCal20 northern hemisphere radiocarbon age calibration curve (0–55 cal kBP). *Radiocarbon* **2020**, *62*, 725–757. [[CrossRef](#)]
53. Karpytchev, Y.A. Reconstruction of Caspian Sea-level fluctuations: Radiocarbon dating coastal and bottom deposits. *Radiocarbon* **1993**, *35*, 409–420. [[CrossRef](#)]

54. Kuzmin, Y.V.; Neveeskaya, L.A.; Krivonogov, S.K.; Burr, G.S. Apparent ^{14}C ages of the 'pre-bomb' shells and correction values (R, ΔR) for Caspian and Aral seas (central Asia). *Nuclear Instr. Meth. Phys. Res.* **2007**, *259*, 463–466. [[CrossRef](#)]
55. Gofman, E.F. *Ecology of Modern and New Caspian Ostracods of the Caspian Sea*; Nauka: Moscow, Russia, 1966; pp. 1–184.
56. Borisova, O.K. Landscape and climatic changes in the Holocene. *Izv. RAS Geogr. Ser.* **2014**, *2*, 5–20. [[CrossRef](#)]
57. Bolikhovskaya, N.S. Evolution of the climate and landscapes of the lower Volga region during Holocene. *Vestnik Mos Univ. Ser. Geogr.* **2011**, *2*, 13–27. [[CrossRef](#)]
58. Richards, K.; Bolikhovskaya, N.; Hoogendoorn, R.; Kroonenberg, S.B.; Leroy, S.A.; Athersuch, J. Reconstructions of deltaic environments from Holocene palynological records in the Volga delta, northern Caspian Sea. *Holocene* **2014**, *24*, 1226–1252. [[CrossRef](#)]
59. Alley, R.B.; Mayevski, P.A.; Sowers, T.; Stuiver, M.; Taylor, K.C.; Clark, P.U. Holocene climatic instability: A prominent, widespread event 8200 yr ago. *Geology* **1997**, *25*, 483–486. [[CrossRef](#)]
60. Makshaev, R.R. Chemical composition of Lower Khvalynian deposits in the Middle and Lower Volga region. In Proceedings of the IGCP 610 and INQUA IFG POCAS, Palermo, Italy, 1–9 October 2017; pp. 118–120.
61. Sudakova, N.G.; Nemtsova, G.M.; Andreicheva, L.N.; Bolshakov, V.A.; Glushankova, N.I. Lithology of the Middle Pleistocene tills in the central and southern Russian Plain. In *Glacial Deposits in North–Eastern Europe*; Ehlers, J., Kozarski, S., Gibbard, P., Eds.; Brookfield: Rotterdam, The Netherlands, 1995; pp. 181–189.
62. Faustova, M.A.; Gribchenko, Y.N. Lithology of glacial deposits of the last Late Pleistocene glaciation. In *Glacial Deposits in North–Eastern Europe*; Ehlers, J., Kozarski, S., Gibbard, P., Eds.; Brookfield: Rotterdam, The Netherlands, 1995; pp. 194–199.
63. Lobacheva, D.M.; Badyukova, E.N.; Makshaev, R.R. Lithofacial structure and conditions of accumulation of Baer knoll deposits in the Northern Caspian region. *Vestnik Mosk. Univ. Ser. 5 Geogr.* **2021**, *6*, 89–101.
64. Zhai, D.; Xiao, J.; Fan, J.; Wen, R.; Pang, Q. Differential transport and preservation of the instars of *Limnocythere inopinata* (Crustacea, Ostracoda) in three large brackish lakes in northern China. *Hydrobiologia* **2014**, *747*, 1–18. [[CrossRef](#)]
65. Kakroodi, A.A.; Leroy, S.A.G.; Kroonenberg, S.B.; Lahijani, H.A.K.; Alimohammadian, H.; Boomer, I.; Goorabi, A. Late Pleistocene and Holocene sea-level change and coastal paleoenvironment evolution along the Iranian Caspian shore. *Mar. Geol.* **2015**, *316*, 111–125. [[CrossRef](#)]
66. Leroy, S.A.G.; Lopes–Merio, L.; Tudryn, A.; Chalié, F.; Gasse, F. Late Pleistocene and Holocene palaeoenvironments in and around the middle Caspian basin as reconstructed from a deep–sea core. *Quat. Sci. Rev.* **2014**, 1–20. [[CrossRef](#)]
67. Wesselingh, F.P.; Neubauer, T.A.; Anistratenko, V.V.; Vinarski, M.V.; Yanina, T.; Poorten, J.J.; Kijashko, P.; Albrecht, C.; Anistratenko, O.Y.; D'Hont, A.; et al. *Mollusc species from the Pontocaspian region—An expert opinion list.* *Zookeys* **2019**, *827*, 31–124. [[CrossRef](#)]
68. Neubauer, T.A.; van de Velde, S.; Yanina, T.A.; Wesselingh, F.P. A late Pleistocene gastropod fauna from the northern Caspian Sea with implications for Pontocaspian gastropod taxonomy. *ZooKeys* **2018**, *770*, 43–103. [[CrossRef](#)]
69. Orlova, M.I.; Therriault, T.W.; Antonov, P.I.; Shcherbina, G.K. Invasion ecology of quagga mussels (*Dreissena rostriformis bugensis*): A review of evolutionary and phylogenetic impacts. *Aquat. Ecol.* **2005**, *39*, 401–418. [[CrossRef](#)]
70. Smith, A.J.; Horne, J.H. Ecology of marine, marginal marine and nonmarine ostracods. In *The Ostracoda. Applications in Quaternary Research*; AGU: Washington, DC, USA, 2002; pp. 37–64. [[CrossRef](#)]
71. Gandolfi, A.; Todeschi, E.B.A.; Rossi, V.; Menozzi, P. Life history traits in *Darwinula stevensoni* (Crustacea: Ostracoda) from Southern European populations under controlled conditions and their relationship with genetic features. *J. Limnol.* **2001**, *60*, 1–10. [[CrossRef](#)]
72. van de Velde, S.; Yanina, T.A.; Neubauer, T.A.; Wesselingh, F.P. The Late Pleistocene mollusk fauna of Selitrennoye (Astrakhan province, Russia): A natural baseline for endemic Caspian Sea faunas. *J. Great Lakes Res.* **2019**, *46*, 1227–1239. [[CrossRef](#)]
73. van de Velde, S.; Wesselingh, F.P.; Yanina, T.A.; Anistratenko, V.V.; Neubauer, T.A.; ter Poorten, J.J.; Vonhof, H.B.; Kroonenberg, S.B. *Mollusc biodiversity in late Holocene nearshore environments of the Caspian Sea: A baseline for the current biodiversity crisis.* *Palaeogeogr. Palaeoclim. Palaeoc.* **2019**, *535*, 109364. [[CrossRef](#)]
74. Makshaev, R.R.; Svitoch, A.A.; Tkach, N.T. Late Pleistocene sedimentation in the Northern Caspian Lowland during the Early Khvalynian transgression. *Limn. Freshw. Biol.* **2020**, *4*, 531–532. [[CrossRef](#)]
75. Velichko, A.A. *Evolutionary Geography: Problems and Decisions*; GEOS: Moscow, Russia, 2012; pp. 1–564.
76. Novenko, E.Y. Changes of Vegetation and Climate Central and Eastern Europe in the Late Pleistocene and the Holocene in Interglacial and Transitional Stages of the Climatic Macrocycles. Ph.D. Dissertation, Moscow State University, Moscow, Russia, 2016; pp. 1–44.
77. Arnoldi, L.I. On the question of the distribution of zoobenthos in the Caspian Sea. In *Materials on Hydrobiology and Lithology of the Caspian Sea*; Publishing House of the Academy of Sciences of the USSR: Moscow, Russia, 1938; pp. 115–171.
78. Karpevich, A.F. Relation of some species of the family Cardiidae to the salt regime of the Northern Caspian. *Dokl. Acad. Sci. USSR New Ser.* **1946**, *54*, 73–75.
79. Zhadin, V.I. *Mollusks of Fresh and Brackish Waters of the USSR*; Publishing House of the Academy of Sciences of the USSR: Moscow, Russia, 1952; pp. 1–376.
80. Neiman, A.A. On the characteristics of the Cardiidae of the Northern Caspian. *Zool. J.* **1959**, *38*, 1891–1893.
81. Shornikov, E.I. Questions of ecology of the Azov–Black Sea ostracods. *Biol. Sea* **1972**, *26*, 53–88.

Disclaimer/Publisher's Note: The statements, opinions and data contained in all publications are solely those of the individual author(s) and contributor(s) and not of MDPI and/or the editor(s). MDPI and/or the editor(s) disclaim responsibility for any injury to people or property resulting from any ideas, methods, instructions or products referred to in the content.